

The subsurface-shear shaped solar $\alpha\Omega$ dynamo

V.V. Pipin¹⁻³ and A.G. Kosovichev³

¹ Institute of Geophysics and Planetary Physics, UCLA, Los Angeles, CA 90065, USA

²Institute of Solar-Terrestrial Physics, Russian Academy of Sciences,

³Hansen Experimental Physics Laboratory, Stanford University, Stanford, CA 94305, USA

Received _____; accepted _____

Abstract

We propose a solar dynamo model distributed in the bulk of the convection zone with the toroidal magnetic field the flux concentrated in the near-surface layer. We show that if the boundary conditions at the top of the dynamo region allow the large-scale toroidal magnetic fields to penetrate closer to the surface, then the pattern of the modelled butterfly diagram for the toroidal magnetic fields in the upper part of the convection zone is formed by the surface rotational shear layer. The model is in agreement with observed properties of the magnetic solar cycle.

Subject headings: Dynamo — Magnetohydrodynamics (MHD) — Sun:dynamo

1. Introduction

It is widely believed that the 11 year sunspot activity is produced and organized by large-scale magnetic fields generated somewhere in the deep convection zone. Most of the solar dynamo models suggest that the toroidal magnetic field that emerges on the surface and forms the sunspots is generated near the bottom of the convection zone (CZ), in the tachocline or just beneath it in overshoot layer, see, e.g., (Choudhuri et al., 1995; Rüdiger & Brandenburg, 1995; Dikpati & Charbonneau, 1999; Bonanno et al., 2002; Tobias & Weiss, 2007). The belief for the deep-seated solar dynamo comes from the fact that this region is sufficiently stable to store magnetic flux despite the magnetic flux-tube buoyancy (Parker, 1975; Spiegel & Weiss, 1980; van Ballegoijen, 1982; Spruit & Roberts, 1983; van Ballegoijen & Choudhuri, 1988; Choudhuri, 1990). The tachocline forms a strong radial shear of the angular velocity. Yet, turbulent diamagnetism (see, e.g., Zeldovich, 1957 or Kitchatinov & Rüdiger, 1992) pumps the magnetic fields from the intensively mixed interior of CZ to its boundaries. This effect can substantially amplify the toroidal magnetic fields near the bottom of CZ, see, e.g., (Krivodubskij, 1987; Guerrero & de Gouveia Dal Pino , 2008).

However, an attention was drawn to the theoretical and observational problems concerning the deep-seated solar dynamo models (Brandenburg, 2005, 2006). The renewed discussion of the place of the solar dynamo can be found, e.g., in papers by Brandenburg (2005) and Tobias & Weiss (2007). In particular, there are some arguments that the near-surface shear of the angular velocity could be important for the solar dynamo distributed in the convection zone. This shear layer becomes an important ingredient of the flux-transport models as well, (see, e.g., Guerrero & de Gouveia Dal Pino , 2008).

In our paper we address the importance of the surface boundary conditions for the surface shear-shaped dynamo models. The commonly used boundary conditions in the solar

dynamo models are the perfect conductor at the bottom of CZ and the vacuum boundary conditions are at the top of the model domain. Both the vacuum and perfect conductor boundary conditions can be regarded as a mathematically convenient idealization. The top boundary conditions at the top plays a particularly important role because it controls the escape of magnetic fields to outside the model domain.

The perfect conductor boundary condition is usually identified as “closed”, (e.g., Choudhuri, 1984), because in this case there is no penetration of the generated magnetic flux outside. For the axi-symmetric magnetic fields all magnetic flux is closed inside the dynamo region. The vacuum boundary condition is identified as "open". In this case the poloidal field lines are open to the outside, and the corresponding magnetic flux “freely” escapes. Also, the strength of the toroidal magnetic field goes smoothly to zero at the boundary. The latter means that the boundary conditions does not allow to the magnetic flux of the toroidal field penetrate to the surface. With such a boundary condition it is hardly possible to form the sunspots from the near-surface large-scale toroidal magnetic fields.

Bearing in mind the dynamical nature of the surface magnetic fields one can model the near-surface behaviour by using a combination of the “open” and “closed” types of the boundary conditions. Various consequences of this idea were explored by (Choudhuri, 1984; Tavakol et al., 1995; Covaset al., 1998; Kitchatinov & Mazur, 1999; Kitchatinov et al., 2000; Tavakol et al., 2002; Käpylä et al. , 2010). Here, we apply this to a solar dynamo model that extends from the bottom of CZ to the top, including the region of the strong near-surface rotational shear. We show that allowing for the toroidal magnetic flux penetrate to the surface brings the butterfly diagrams of the toroidal large-scale magnetic field (LSMF) in the upper part of CZ, and the phase relations between the different components of the dynamo-generated magnetic field LSMF in agreement with the solar cycle observations.

2. Dynamo equations

The evolution of the axi-symmetric magnetic field (B being the azimuthal component of the magnetic field, A is proportional to the azimuthal component of the vector potential) is governed by the following equations:

$$\frac{\partial A}{\partial t} = r \sin \theta \mathcal{E}_\phi \quad (1)$$

$$\begin{aligned} r \sin \theta \mathcal{E}_\phi &= \psi_\eta \eta_T \left\{ f_2^{(d)} + 2f_1^{(a)} \right\} \frac{\partial^2 A}{\partial r^2} + \psi_\eta \eta_T \left\{ f_2^{(d)} + 2f_1^{(a)} \right\} \frac{(1 - \mu^2)}{r^2} \frac{\partial^2 A}{\partial \mu^2} + \\ &+ \psi_\alpha C_\alpha \eta_T G f_{12}^{(a)} r \mu \sin \theta f(\theta) B \\ &+ G \left(2f_1^{(a)} \mu \sin^2 \theta \frac{\partial A}{\partial \mu} - \left(f_3^{(a)} - f_1^{(a)} \sin^2 \theta \right) \frac{\partial A}{\partial r} \right) \end{aligned} \quad (2)$$

$$\frac{\partial B}{\partial t} = -\sin \theta \left(\frac{\partial \Omega}{\partial r} \frac{\partial A}{\partial \mu} - \frac{\partial \Omega}{\partial \mu} \frac{\partial A}{\partial r} \right) + \frac{1}{r} \frac{\partial r \mathcal{E}_\theta}{\partial r} + \frac{\sin \theta}{r} \frac{\partial \mathcal{E}_r}{\partial \mu} \quad (3)$$

$$\begin{aligned} \mathcal{E}_r &= \frac{\eta_T \psi_\eta}{r} \left\{ \left(f_2^{(d)} + 2f_1^{(a)} (1 - \mu^2) \right) \frac{\partial \sin \theta B}{\partial \mu} \right. \\ &\quad \left. + 2f_1^{(a)} \mu \sin \theta \frac{\partial}{\partial r} r B + 2r G f_1^{(a)} \mu \sin \theta B \right\} \end{aligned} \quad (4)$$

$$\begin{aligned} r \mathcal{E}_\theta &= \eta_T \psi_\eta \left\{ \left(f_2^{(d)} + 2f_1^{(a)} \mu^2 \right) \frac{\partial r B}{\partial r} + \right. \\ &\quad \left. + 2f_1^{(a)} \mu \sin \theta \frac{\partial}{\partial \mu} (\sin \theta B) \right. \\ &\quad \left. - r G \left(f_1^{(a)} \cos 2\theta + f_3^{(a)} \right) B \right\} \end{aligned} \quad (5)$$

The given system of equations is similar to that used by Pipin & Seehafer (2009) and Seehafer & Pipin (2009). We use the same notations for the functions and parameters as those introduced by Pipin (2008) (hereafter, P08). Here, $G = \partial_r \log \rho$ is the density stratification scale. Functions $f_{1,2,12}^{(a,d)}$ depend on the Coriolis number $\Omega^* = 2\tau_c \Omega_0$; functions $\phi_6^{(a)}$ and $\psi_{\eta,\delta}$ describe magnetic quenching and depend on $\beta = B/\sqrt{\mu_0 \rho u^2}$; parameter C_α controls the contributions of the α effects. Similar to Dikpatiet al. (2004) we confine the

alpha-affect in Eq.(2) at low latitude by specifying:

$$\sin \theta f(\theta) = \left(1 + e^{30(|\theta - \pi/2| - \pi/6)}\right)^{-1}. \quad (6)$$

The radial dependence of the alpha-effect is defined by the density stratification factor G and the function of the Coriolis number $f_{12}^{(a)}(\Omega^*)$, that is given in P08. In notations of P08, $\psi_\eta = \phi_3 + \phi_2 - 2\phi_1$. We introduce parameter C_η to control the turbulent diffusion coefficient, $\eta_T = C_\eta \eta_T^{(0)}$ and $\eta_T^{(0)} = \tau_c \bar{u}^2/3$. The internal parameters of the solar convection zone are given by Stix (2002). In vicinity of the top of solar convection zone the stratification is strongly deviates from the adiabatic one also the turbulence parameters varies sharply in approaching to the surface. For this reasons we confine the integration domain from $0.71R_\odot$ to $0.972R_\odot$ in radius, and from the pole to the pole in latitude. The differential rotation profile, $\Omega = \Omega_0 f_\Omega(x, \mu)$ (shown on the Fig.1) is a slightly modified version proposed by Antia et al. (1998):

$$\begin{aligned} f_\Omega(x, \mu) &= \frac{1}{\Omega_0} (\Omega_0 + 55(x - .7) \phi(x, x_0) \phi(-x, -.96) \\ &\quad - 200(x - .95) \phi(x, .96)) \\ &\quad + (21P_3(\mu) + 3P_5(\mu)) \left(\frac{\mu^2}{j_p(x)} + \frac{1 - \mu^2}{j_e(x)} \right) / \Omega_0 \\ j_p &= \frac{1}{1 + \exp\left(\frac{.709 - x}{0.02}\right)}, \quad j_e = \frac{1}{1 + \exp\left(\frac{.692 - x}{0.01}\right)} \end{aligned} \quad (7)$$

where Ω_0 is the equatorial angular velocity of the Sun at the surface, $x = r/R_\odot$, $\phi(x, x_0) = .5 [1 + \tanh[100(x - x_0)]]$, $x_0 = 0.71$. The distribution of the Coriolis number, turbulent diffusivity and the rms convection velocity are shown at the middle on Fig.1. The radial profile of the alpha-effect is shown on the right panel there.

For the bottom of the integration domain we apply the perfect conductor ("closed") boundary conditions: $\mathcal{E}_\theta = 0$, $A = 0$. The boundary conditions at the top are defined as following. Bearing in mind the ideas given in Introduction, we introduce a parameter δ to switch between the “open” and the “closed” boundary conditions at the top. For the toroidal

field we use the similar type of condition as discussed by Kitchatinov et al. (2000).

$$\delta \frac{\eta_T}{r_e} B + (1 - \delta) \mathcal{E}_\theta = 0. \quad (8)$$

For the poloidal field we apply a combination of the local condition $A = 0$ and conditions of smooth transition from the inner poloidal field to the potential field in the outside domain:

$$\delta \left(\frac{\partial A}{\partial r} \Big|_{r=r_e} - \frac{\partial A^{(vac)}}{\partial r} \Big|_{r=r_e} \right) + (1 - \delta) A = 0, \quad (9)$$

where the potential field in the outside domain is

$$A^{(vac)}(r, \mu) = \sum a_n \left(\frac{r_e}{r} \right)^n \sqrt{1 - \mu^2} P_n^1(\mu), \quad (10)$$

where, $P_n^1(\mu)$ is the associated Legendre polynomials. The numerical implementation of (9) is as following. Take the one-side difference approximation for the radial derivative:

$$\frac{\partial A_j}{\partial r} \Big|_{r=r_e} = \frac{3A_{Nj} - 4A_{N-1j} + A_{N-2j}}{2h_r}$$

and consider the decomposition (10) at the top $r = r_e$, $A_{Nj} = \sum a_n \sqrt{1 - \mu_j^2} P_n^1(\mu_j)$. Then, define matrices $M_{nj}^{(a)} = \sqrt{1 - \mu_j^2} P_n^1(\mu_j)$ and $\tilde{M}_{jn} = n \sqrt{1 - \mu_j^2} P_n^1(\mu_j)$, with μ_j computed in collocation points of P_n^1 . This procedure allows us to express the spectral coefficients in (10) via the known values of the potential, A , at the nodes, $a_n = M_{nj}^{(a)-1} A_{Nj}$. Substituting this in Eq.(9) and solving it we get :

$$A_{Nj} = \delta \left(3E_{jk} + 2h_r \tilde{M}_{jk} M_{nk}^{(a)-1} \right)^{-1} (4A_{N-1jk} - A_{N-2k}),$$

where E is a unit diagonal matrix.

3. Results and discussion

Parameter δ in the boundary conditions describes a transition from the “closed” ($\delta = 0$) to “open” ($\delta = 1$) cases. Physically, it controls penetration of the dynamo-generated fields into the outer atmosphere.

Decreasing δ in Eqs.(8,9) results in the stronger tangential- and the weaker radial large-scale magnetic fields at the surface. While the strong toroidal magnetic field is a welcome feature of the model, the weak radial magnetic field decrease the efficiency of the radial subsurface shear to produce large-scale toroidal magnetic fields. In fact, the simulations reveal that the critical dynamo number, C_α , is growing when the penetration parameter δ . By this reason we restrict ourselves by the case of a small deviation of the boundary conditions from the vacuum ("open") conditions. Moreover, to match the dynamo period to the solar cycle we choose the magnetic diffusivity parameter $C_\eta = 0.05$, which is significantly lower then value predicted by the mixing length theory. To demonstrate the effect of the new boundary conditions with the field penetration we show for comparison the results for two runs in Figure 2 and 3. In one run, we apply $\delta = 0.95$ (partial penetration) and in another - $\delta = 1$ (the vacuum boundary conditions). The results are shown at the Fig. 2 and Fig. 3 respectively.

Our results show that allowing the large-scale toroidal magnetic field penetrate in to the surface layers changes the direction of the latitudinal migration of the toroidal field activity and produces the magnetic butterfly diagram in close agreement with the solar-cycle observations. The dynamo-wave penetrates to the surface and propagates along the iso-surface of angular velocity. It is in agreement with the Yoshimura rule (Yoshimura, 1975). Both of the presented runs were started with the initial magnetic fields of the equally mixed parity. The evolution retains only the dipole-like parity configurations in both cases though the relaxation time in the penetration case of $\delta = 0.95$ is much longer than in the case of the pure vacuum boundary conditions. If we relax the confinement of the alpha-effect in latitude, i.e., $f(\theta) = 1$ instead of Eq.(6), the general patterns of the Fig.2 are hold except that the maximum of the toroidal LSMF are shifted to higher latitude $\approx 32^\circ$. Therefore we can conclude that the $\alpha\Omega$ - dynamo model with the boundary conditions which allows a small partial penetration of the toroidal field in the outer layers,

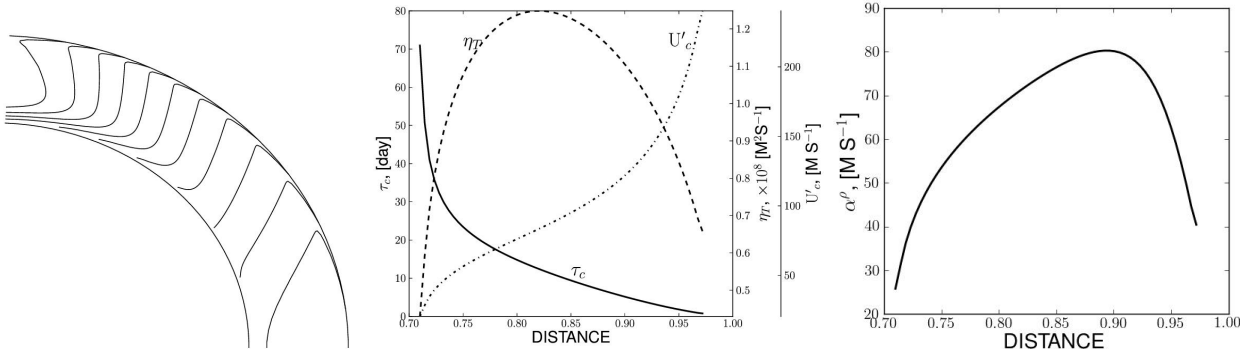


Fig. 1.— Left, the differential rotation law, middle - the turnover convection time, τ_c , turbulent diffusivity, η_T , RMS convective velocity, u'_c , right - the radial profile of the alpha-effect, which is calculated by $\alpha^\rho = \eta_T G f_{12}^{(a)}(\Omega^*)$, see Eq.(2).

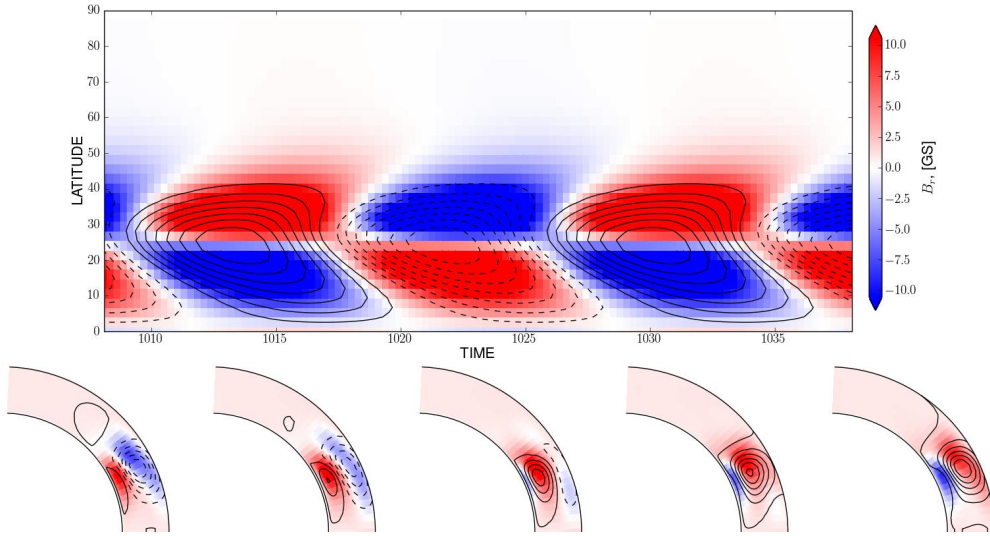


Fig. 2.— The case of $\delta = 0.95$ (top boundary conditions with penetration of magnetic fields). The top panel shows the near-surface toroidal component of large-scale magnetic fields (contour lines) and the surface radial component of the field (color background). The bottom panel shows snapshots of the magnetic field poloidal (contour lines) and toroidal components for a half of the magnetic cycle. The maximum strength of the toroidal LSMF is about 1KG. Time is in years.

robustly reproduce the solar-like butterfly diagram of the near-surface large-scale magnetic field evolution. These results demonstrate of importance of the subsurface rotational shear layer in the solar dynamo mechanism.

4. Acknowledgements

This work was supported by NASA LWS NNX09AJ85G grant and partially by RFBR grant 10-02-00148-a.

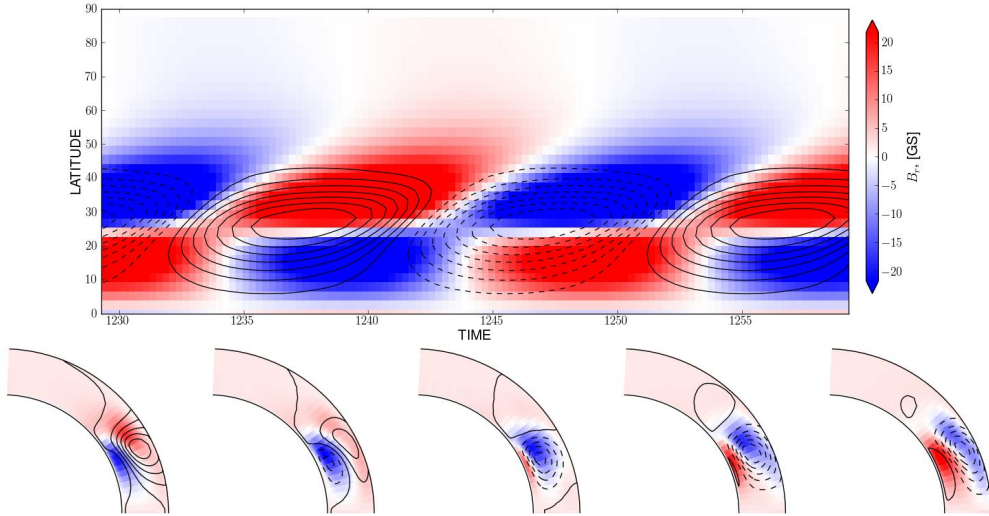


Fig. 3.— The same as in on the Fig.2 for the vacuum boundary conditions, $\delta = 1$.

REFERENCES

- Antia, H. M. , Basu, Sarbani, Chitre, S. M. 1998, MNRAS, 298,543
- Brandenburg, A. 2006, ASP Conference Series, 354,Solar MHD Theory and Observations:
A High Spatial Resolution Perspective, 121
- Brandenburg, A.,2005, Ap.J., 625, 539
- Brandenburg, A., Subramanian, K..2005, Phys. Rep. 417, 1
- Bonanno, A., Elstner, D., Rüdiger, G., 2002, A&A, 390, 673
- Choudhuri, A. R., Schüssler, M., & Dikpati, M. 1995, A&A, 303, L29
- Choudhuri, A. R. 1984, ApJ, 281, 846
- Choudhuri, A. R. 1990, ApJ, 355, 733
- Covas, E., Tavakol, R., Tworkowski, A., Brandenburg, A. 1998, A & A, 329, 350
- Dikpati, M., & Charbonneau, P. 1999, ApJ, 518, 508
- Dikpati, M., de Toma, G., Gilman, P.A., Arge, C.N., White, O.R. 2004, ApJ,601,1136
- Guerrero, G., de Gouveia Dal Pino, E. M. 2008, A& A, 485, 267
- Käpylä, P.J., Korpi, M.J. & Brandenburg, A. 2010, A& A, 518, 22
- Kitchatinov, L.L., Rüdiger, G. 1992, A & A,260, 494
- Kitchatinov, L.L., Mazur, M.V. 1999, AstL,25, 471
- Kitchatinov, L. L., Mazur, M. V., Jardine, M., A& A, 359, 531
- Kitchatinov, L.L., Pipin, V.V. 1993, A& A, 274, 647

- Krivodubskij, V. N., 1987, SvAL,13, 338
- Moss, D. , Brooke, J., 2000, MNRAS, 315,521
- Parker, E.N., 1975, ApJ, 198, 205
- Pipin, V.V. & Seehafer, N. 2009, A&A, 493,819
- Pipin, V. V. 2008, Geophys. Astrophys. Fluid Dynam., 102, 21
- Rüdiger, G., Brandenburg, A., 1995, A& A, 296, 557
- Seehafer, N. & Pipin, V.V. 2009, A&A, 508,9
- Spiegel, E.A., & Weiss, N.O., 1980, Nature, 287, 616
- Spruit, H.C., & Roberts, B., 1983, Nature, 304, 401
- Stix, M. 2002, The Sun. An Introduction, 2nd Ed. (Berlin: Springer)
- Tavakol, R.K., Tworkowski, A. S., Brandenburg, A., Moss, D., Tuominen, I., 1995, A& A, 296, 269
- Tavakol, R.; Covas, E.; Moss, D.; Tworkowski, A. 2002 A & A, 387, 1100
- Tobias, S. & Weiss, N. 2007, in “The Solar Tachocline”, eds by Hughes,D.W., Rosner, R. and Weiss N.O., CUP, Cambridge, UK, p.319
- van Ballegooijen, A. A. 1982, A & A, 113, 99
- van Ballegooijen, A.A., Choudhuri, A.R. 1988, ApJ, 333, 965
- Zeldovich, Ya.B. 1957, Sov.Phys. JETP, 4, 460
- Yoshimura, H. 1975 ApJ, 201, 740